

## Research Article

# The Research of Mathematical Method and Position Control of Actuator in Power Switchgear

Enyuan Dong,<sup>1</sup> Taotao Qin,<sup>1</sup> Yushuo Chen,<sup>1</sup> Hang Su,<sup>2</sup> and Jiyan Zou<sup>1</sup>

<sup>1</sup> Department of Electrical and Electronics Engineering, Dalian University of Technology, Dalian 116024, China

<sup>2</sup> Department of College of Electromechanical and Information Engineering, Dalian Nationalities University, Dalian 116024, China

Correspondence should be addressed to Enyuan Dong; dey2000@tom.com

Received 3 April 2013; Revised 29 June 2013; Accepted 8 July 2013

Academic Editor: Rongni Yang

Copyright © 2013 Enyuan Dong et al. This is an open access article distributed under the Creative Commons Attribution License, which permits unrestricted use, distribution, and reproduction in any medium, provided the original work is properly cited.

Transient effects such as overvoltage and inrush currents will be caused due to opening and closing the switchgear at random phase. Phase-controlled technology present in recent years, which is restricted by the operation dispersion of actuator, can limit the transient effects. And the dispersion of the switchgear with a permanent magnetic actuator (PMA) is small. Therefore, the research of mathematical method and position control in this paper is based on the PMA. Firstly, the dynamic mathematical method and simulation system established in MATLAB are used to improve the design of the PMA owing same type. Secondly, simulation with the use of improved fuzzy algorithm is carried out. And an optimized self-adaptive fuzzy algorithm is obtained in the simulation process which can be used to trace the given displacement curve. Finally, a large number of tracing experiments have been done on the 35 kV breaker prototype to verify the effectiveness of the algorithm. In the experiments, the closing time of breaker can be stabilized within  $\pm 0.5$  ms when capacitor voltage and capacitance change. These results prove that the mathematical model and the fuzzy algorithm are effective and practical.

## 1. Introduction

Phase-controlled technology [1, 2], which has become an increasingly useful method to decrease the high inrush current and overvoltage in power system, is opening or closing circuit breaker at the optimal phase of current or voltage. As the precision of synchronous switch depends on the closing and opening time dispersions, the stability of the actuator becomes pivotal. PMA, which acts stably and can be controlled very well, is suitable for vacuum circuit breaker. However, the stability of PMA changes with external factors such as capacitor voltage and capacitance. In this paper, the variation of displacement curve is collected and analyzed in real time, and the controller gives a relevant command to trace the given displacement curve. It achieves the speed control in real time and ensures the precise control of synchronous switch.

In this paper, the dynamic model of monostable PMA is established. And the pulse width modulation (PWM)

technology and fuzzy adaptive algorithm are applied in the closed-loop system in which free-wheeling process of coil has been taken into consideration. The details of the system will be described in the following part. Displacement value of actuator is collected real time with a linear displacement sensor. And displacement deviation can be obtained by comparing the collected value with the given standard curve. Duty cycle of PWM is then adjusted by the fuzzy controller according to displacement deviation and the changing rate of deviation. Thus, coil current will be changed in accordance with the duty cycle of PWM, and then the velocity of actuator can be adjusted. The results of simulation in MATLAB with different capacitor voltages prove that the given curve can be traced well with the control method. In addition, a large number of tracing experiments have been done on the 35 kV breaker prototype when capacitor voltage and capacitance change. DSP2812 is used in the hardware system. The experimental results show that the closing time of breaker can be

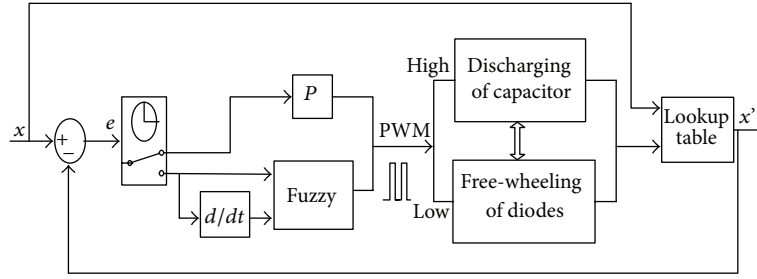


FIGURE 1: Structure of control system for PMA.

stabilized within  $\pm 0.5$  ms and the control algorithm is effective and feasible.

## 2. Structure and Analysis of the System

**2.1. Structure of the System.** In this paper, a closed-loop control [3–8] method is used to realize the adaptive control of system. Dynamic process of PMA can be divided into two stages according to the state of the core: one is exciting stage of coil current and the other is moving stage of core. Fuzzy control algorithm and proportional control method are adopted in this system. Proportional control is used to trace the standard current in exciting stage, while fuzzy control is used to trace the standard displacement in moving stage. There is a switch, whose time is determined by the exciting time of the coil, to select the two stages above.

A displacement sensor and a hall sensor are used to measure the current and displacement data. And the real-time data are sent to AD sampling module in DSP. By comparing real-time data with the given value of standard curve, the deviation of the displacement of core can be found. Then, the deviation  $e$  is calculated by the control algorithm, and the controller outputs a different duty cycle of the PWM pulse to drive the IGBT. Finally, IGBT is switched on and off to control the discharge of the capacitor, so that the speed of the moving core is controllable. The structure of the whole system is shown in Figure 1.

**2.2. Analysis of the System.** The general structure of the system is shown in Figure 2. Direct current is supplied for the coil by the precharged capacitors. Bridge circuit, consisting of four IGBTs, is used to realize PWM control of the monostable PMA. The basic model of the system is found based on voltage balance equation of the electromagnet coil which produces electromagnetic force to drive the actuator:

$$U_c(t) = i(t) * r + \frac{d\psi(t)}{dt}, \quad (1)$$

$$\frac{dU_c(t)}{dt} = -\frac{i(t)}{c}.$$

In the balance equations [9–13] above,  $U_c(t)$  is the voltage of the capacitor,  $r$  is the resistance of the coil,  $\psi(t)$  is the magnetic flux of coil,  $i(t)$  is the discharging current of circuit, and  $c$  is the capacitance.

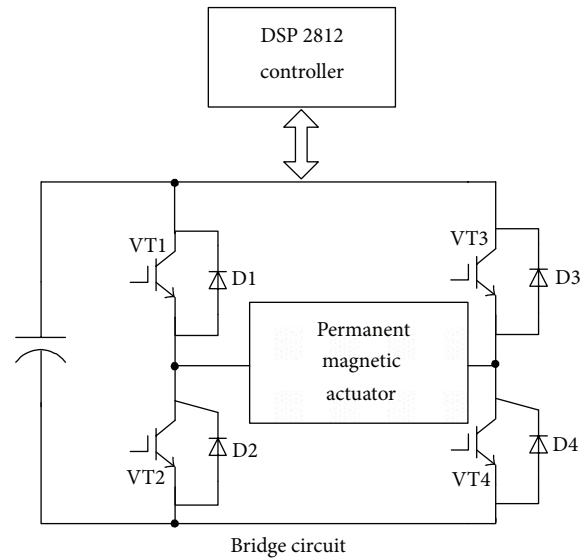


FIGURE 2: Schematic diagram of monostable PMA and the bridge circuit.

In the closing process of the circuit breaker, VT1 and VT4 are triggered when the PWM controller outputs a high level. Then, the capacitor discharges through the IGBT to the coil whose inductance generates a reverse electromotive force  $E$ . As is shown in Figure 3(a), equivalent electric circuit resulted according to Kirchhoff's Laws.

VT1 and VT4 are turned off when the PWM control circuit outputs a low level and the free-wheeling diodes D2 and D3 are conducted. Original direction of the current can still be maintained for a while because of the coil inductance. Yet the direction of electromotive force will change. Thus, the energy stored in the coil inductance feeds back to the capacitor through the free-wheeling circuit. This free-wheeling process results in the increase of capacitor voltage. Equivalent circuit is shown in Figure 3(b), and the voltage balance equation is shown below:

$$-\frac{d\psi(t)}{dt} = U_c(t) + i(t) * r, \quad (2)$$

$$\frac{dU_c(t)}{dt} = \frac{i(t)}{c}.$$

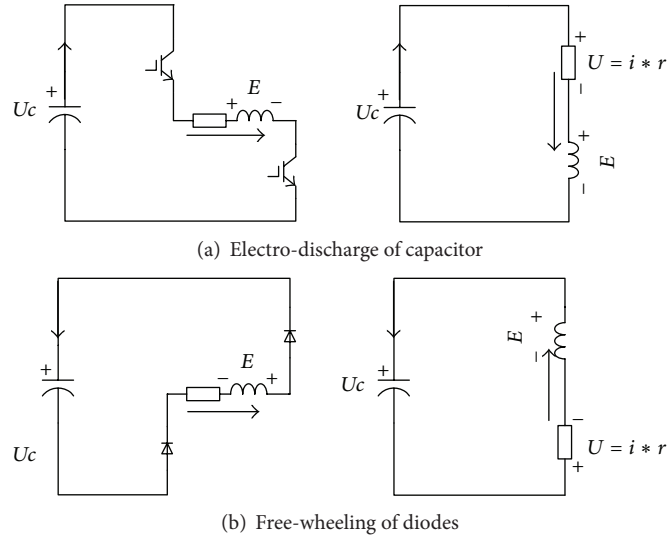


FIGURE 3: Simplified circuit of bridge circuit.

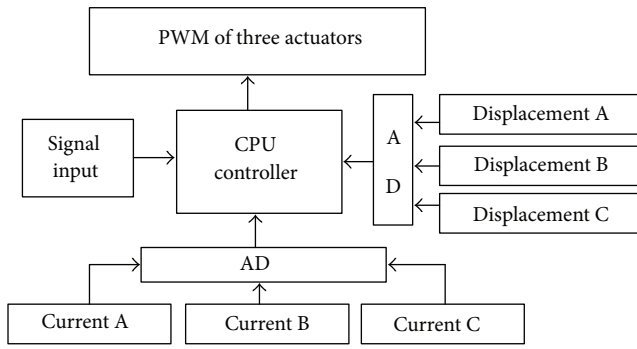


FIGURE 4: Hardware structure of the system.

Both the electromagnetic parameters and mechanical parameters of the actuator change when the core moves. Newton's law is used to analyze the dynamic process. These equations of discharging process and free-wheeling process are shown as follows.

Discharging process:

$$\begin{aligned} \frac{d\psi(t)}{dt} &= U_c(t) - Ri(t), \\ \frac{dv(t)}{dt} &= \frac{F(t) - F_f(t)}{m}, \\ \frac{dx(t)}{dt} &= v(t), \\ \frac{dU_c(t)}{dt} &= -\frac{i(t)}{c}. \end{aligned} \quad (3)$$

Free-wheeling process:

$$\begin{aligned} \frac{d\psi(t)}{dt} &= -U_c(t) - Ri(t), \\ \frac{dv(t)}{dt} &= \frac{F(t) - F_f(t)}{m}, \end{aligned}$$

$$\begin{aligned} \frac{dx(t)}{dt} &= v(t), \\ \frac{dU_c(t)}{dt} &= \frac{i(t)}{c}. \end{aligned} \quad (4)$$

**2.3. Hardware Structure of the System.** The hardware structure is shown in Figure 4. In CPU controller module, DSP2812 is the core of hardware system. When motion commands are given by signal input module, CPU will control the breaker closing or opening. A breaker has three phases, including phase A, B, and C, so the system comprises three displacement sensors and three hall current sensors. Linear displacement sensor is used to collect displacement value of actuator. Hall current sensor is used to collect the current value. Current and displacement signals are converted into an electric signal by sensors. In AD module, a semiconductor chip collects the current and displacement values. AD means that the analog value is transformed to digital value. The data is received and processed by CPU controller. Variable PWM of CPU controller is outputted after the data is calculated in 2812 with the algorithm.

### 3. Control Algorithm

**3.1. Proportional Control Method.** In the current exciting stage, the current data is acquired. The formula is shown below:

$$I_{out}(n) = kp * (I(n) - I(n-1)), \quad (5)$$

where  $I(n)$  is the current data acquired at the  $n$  moment by current hall sensor,  $I(n-1)$  is the current data at the  $(n-1)$  moment, and  $I_{out}(n)$  is the output duty cycle of PWM at the  $n$  moment.

**3.2. Fuzzy Algorithm with a Self-Adjustment Function.** In the traditional fuzzy control method, an offline fuzzy controller

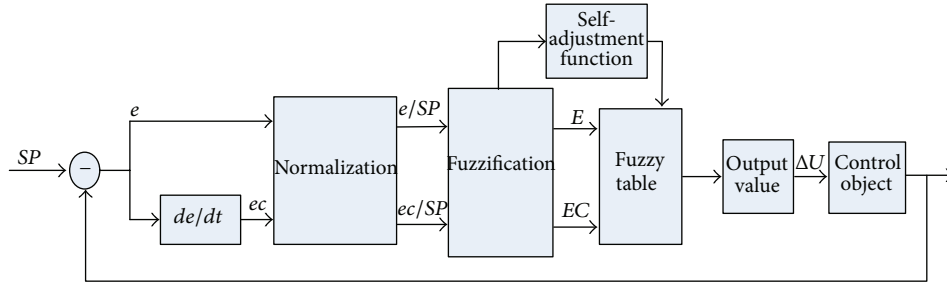


FIGURE 5: Fuzzy controller schematic diagram.

polling list, which is calculated by the computer, is used to quantify the  $e$  and  $ec$  into the polling list. According to the quantized result, corresponding output value is obtained. The disadvantage of the method is that the value of the fuzzy controller polling list is constant. It means that the weighted value cannot be changed. This method cannot meet the demand of the circuit breaker control. In this paper, fuzzy algorithm [14–18] with a parameter self-adjustment function is adopted and described as follows.  $\alpha$  is the weighting factor with which the polling list can be adjusted in real time. When deviation  $e$  is large, the output energy should be increased to decrease the deviation as quickly as possible. When deviation  $e$  is small and the  $de/dt(ec)$  is large in the process, the system must go into steady state as quickly as possible. In addition, in order to avoid the oscillation when the given displacement value is approached, the integration part shown in formula (11) is brought in. Here, the deviation  $e$  is the difference between measured displacement and given standard displacement. The  $de/dt(ec)$  is the changing rate of deviation  $e$ . The parameter self-adjustment function is shown below:

$$\alpha = k * \left| \frac{e}{SP} \right|, \quad (6)$$

$$e(n) = s(n) - s(n-1), \quad (7)$$

$$ec(n) = s(n) - 2s(n-1) + s(n-2). \quad (8)$$

In formula (6),  $\alpha$  is the weighting factor and its value changes with the deviation  $e$  which varies every moment,  $k$  is a constant parameter which is selected through large number of experiments, and  $SP$  is the given value of the breaker stroke.  $s(n)$  is the displacement value at the  $n$  moment,  $s(n-1)$  and  $s(n-2)$  are the displacement values at  $n-1$ ,  $n-2$  moments. From (7) and (8), the whole displacement is discrete. According to formula (6), fuzzy rule can be adjusted continuously with the change of deviation  $e$ . This method overcomes the disadvantage that output value  $\alpha$  is constant and the fuzzy rule could not be adjusted itself. Considering the oscillation phenomena when the given curve is approached, the integral is brought in the algorithm. The fuzzy rules are determined by the following formula:

$$E = k1 * e, \quad (9)$$

$$EC = k2 * ec, \quad (10)$$

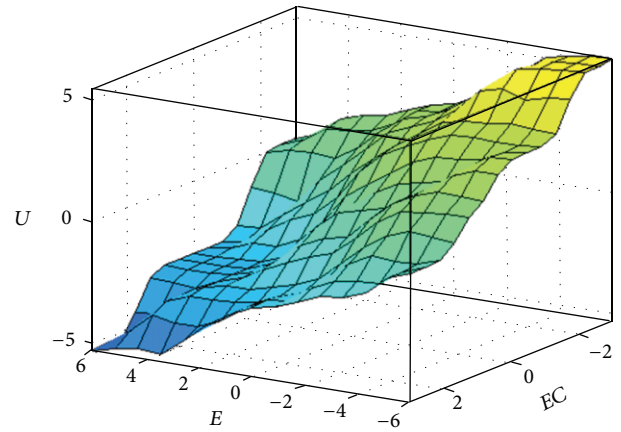


FIGURE 6: Surface of fuzzy rules in fuzzy controller.

$$\Delta U = \begin{cases} \alpha E & E > E1 \\ \alpha E + (1 - \alpha) EC & E2 < E < E1 \\ \alpha E + (1 - \alpha) EC + \beta \sum E & E < E2, \end{cases} \quad (11)$$

$$u = k3 * \Delta U, \quad (12)$$

$$U = U0 + u, \quad (13)$$

where  $E$  is the fuzzy value of deviation  $e$ .  $EC$  is the fuzzy value of deviation variation  $de/dt$ ,  $U$  is the sum of  $U0$  and  $u$ , and  $U0$  is the basic duty cycle obtained by switching characteristics tester.  $k1$ ,  $k2$ , and  $k3$  are quantization factors which can quantify practical deviation into language variable domain.  $\beta$  is the integral coefficient of deviation  $E$ ,  $\Delta U$  is the fuzzy output value,  $u$  is actual output value, and  $E1$  and  $E2$  are the thresholds of deviation  $E$ . According to the experimental results, the parameters  $E1$ ,  $E2$ ,  $\alpha$ , and  $\beta$  will change until these parameters can adapt the variation of external factors such as capacitor voltage and capacitance. So the algorithm is intelligent. The schematic diagram is shown in Figure 5.

Deviation  $e$  and  $ec$  are quantified into seven grades in this paper. The fuzzy rules form Table 1 and the surface of fuzzy rules in fuzzy controller are shown in Figure 6.

**3.3. Simulation Model and Analysis.** Ansoft Maxwell is used in simulation to achieve static magnetic field analysis of PMA.

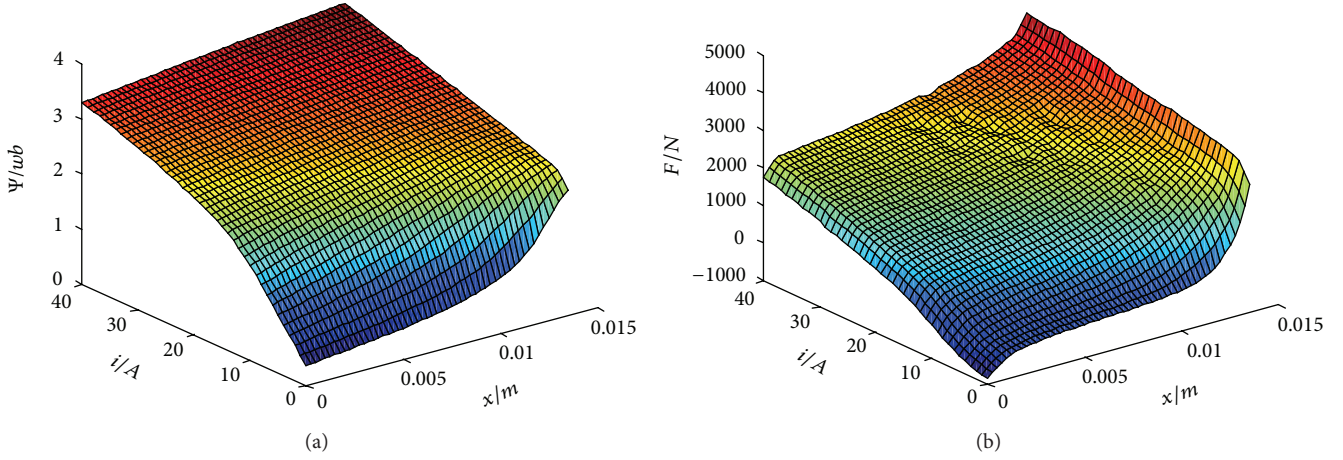


FIGURE 7: Function libraries of the flux linkage and electromagnetic force.

TABLE 1: Fuzzy rule table.

$\Delta U$	$E$						
	NB	NM	NS	ZO	PS	PM	PB
EC							
NB	PB	PB	PM	PM	PS	ZO	NS
NM	PB	PB	PM	PS	PS	ZO	NS
NS	PM	PM	PM	PS	ZO	NS	NS
ZO	PM	PM	PS	ZO	NS	NM	NM
PS	PS	PS	ZO	NS	NS	NM	NM
PM	PS	ZO	NS	NM	NM	NM	NB
PB	ZO	ZO	NM	NM	NM	NB	NB

From the formula (14) and (15), function libraries of magnetic flux and electromagnetic force of core are obtained:

$$\psi(t) = \psi(x(t), i(t)), \quad (14)$$

$$F(t) = F(x(t), i(t)). \quad (15)$$

The static function libraries, which are shown in Figure 7, are prepared for the function call in simulation. The curved surface is different for different operating mechanisms. In this paper, the curved surface is suitable for 35 kV circuit breaker.

According to the conclusion above, simulation model of the system in MATLAB is drawn in Figure 8. One-dimensional interpolation and two-dimensional interpolation are used to calculate the electromagnetic force and the coil flux of PMA. The resistance of friction and spring force at different displacements is given by a one-dimensional interpolation function. The current  $i$  is calculated by the displacement  $x$  in the subsystem.

The speed regulation of PMA aims at the target that closing time of circuit breaker remains unchanged in different circumstances such as capacitor voltage, and capacitance. In the simulation of this paper, experiential and reasonable standard curves are given at the capacitor voltage of 300 V. The blue curves in Figure 9 are the standard displacement curve and coil current curve. The red curves are obtained by

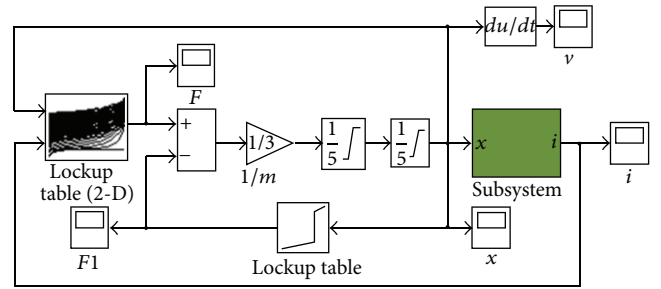


FIGURE 8: Simulation model of closed-loop control system of PMA during closing process.

the control algorithm. It seems that the standard curves are traced well in the figure.

A series of simulations under different capacitor voltages have been done in the simulation system. Displacement deviation shown in Figure 10 is calculated at the voltage of 280 V, 290 V, 310 V, and 320 V. From these curves, it can be seen that closing time of the breaker varies within 0.2 ms when the voltage changes in the range of  $\pm 20$  V. The control algorithm is effective and feasible.

## 4. Experiments

Based on the previous theory and algorithm, a large number of tracing experiments have been done. And the standard curve is followed on prototype when capacitive voltage and capacitance change. The displacement of PMA can be divided into two parts: opening travel and super path. In the following diagram, the whole distance is 22 mm, in which the value of opening travel is 18 mm. The rest of the part beyond this value is no longer considered for the reason that contacts of the breaker have been closed.

**4.1. Experiment of Mutative Voltage.** Experiments have been carried out on prototype when the capacitor voltage changes. The capacitor voltage changes at intervals of 10 V in the



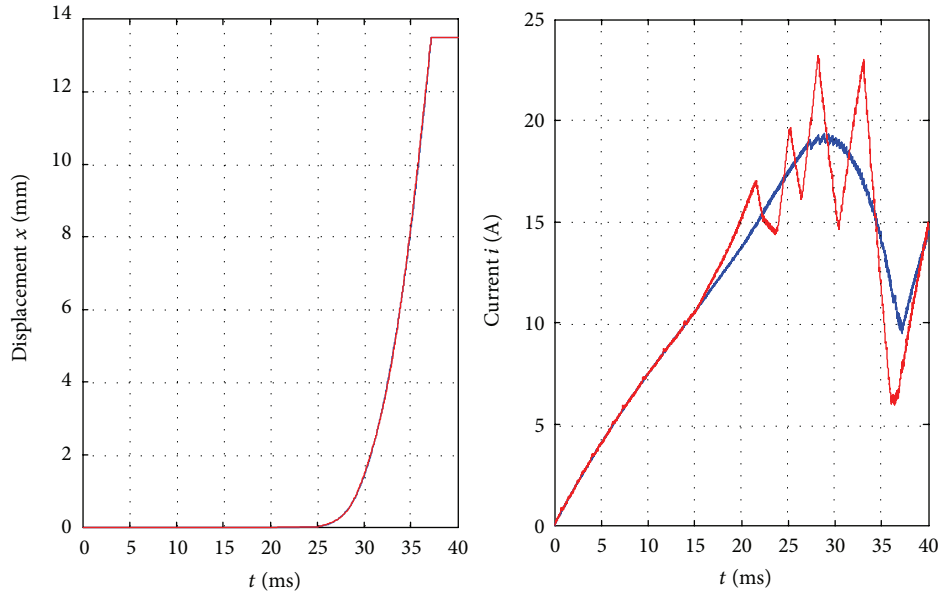


FIGURE 9: The tracing result at the voltage of 320 V.

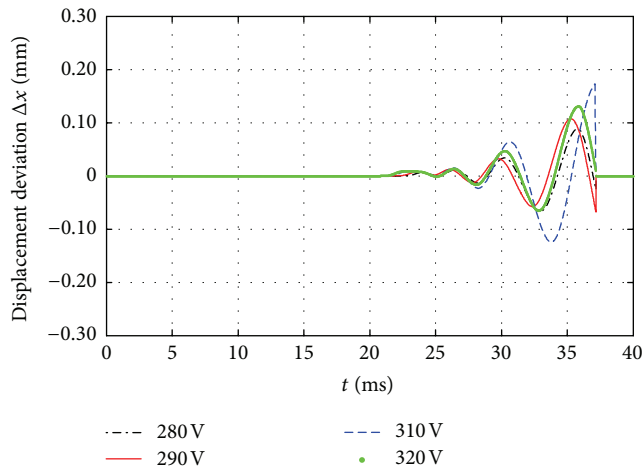


FIGURE 10: The displacement deviation of PMA under different voltages.

range of 190 V to 230 V. Displacement curves in Figure 11 are obtained without of the controlling algorithm. By the  $P$  and fuzzy algorithms in the system, curves in Figure 12 are obtained. In Figure 12, it seems that the whole moving process of the actuator is traced well when voltage changes and the mechanical properties of actuator can keep optimal by  $P$  and fuzzy algorithms. In other words, speed of actuator can be controlled while every displacement point is approached well. The closing time is shown in Table 2. From the data in Table 2, the maximum deviation of time is 10 ms without adjustment. For the relationship between the capacitor power and the square of voltage is linear, the capacitor power varies much when capacitor voltage changes slightly. It is difficult to correct the displacement deviation caused by changes of voltage. However, the closing time is reduced within

TABLE 2: Closing time in different voltages (ms).

	190 V	200 V	210 V	220 V	230 V
Without control	48.66	45.22	42.53	40.57	38.69
Control	48.26	48.16	48.26	48.45	48.55

TABLE 3: Closing time in different capacitances (ms).

	15000 uf	18000 uf	21000 uf	24000 uf	27000 uf	30000 uf
Without control	45.05	44.10	43.33	42.96	42.69	42.48
Control	50.86	50.72	50.97	50.57	50.40	50.46

$\pm 0.5$  ms by the use of the algorithm. Closing time dispersion is decreased largely, and the accuracy of phase-controlled operation is also improved.

**4.2. Experiment of Mutative Capacitance.** Experiments have been carried out on prototype one when capacitance changes at intervals of 3000 uf. Displacement curves in Figure 13 are obtained without PD and fuzzy algorithm. By the use of the algorithm, curves in Figure 14 are obtained. Curves in Figures 13 and 14 show the whole stroke of actuator. It is about 22 mm. In Figure 14, we can see that the whole movement process of the actuator is traced well when capacitance changes. In Table 3, there are two groups of data showing the closing time of breaker: one is with the control of algorithm and the other is without control of algorithm. From the data in Table 3, the maximum deviation of time is 2.57 ms without adjustment. The deviation is reduced to 0.5 ms by the use of the algorithm. We can also find that the impact to the closing time decreased with the increasing of the capacitance. It is for the reason that the output power is insufficient when the capacitance is large enough. But in fact, when the capacitance increases to

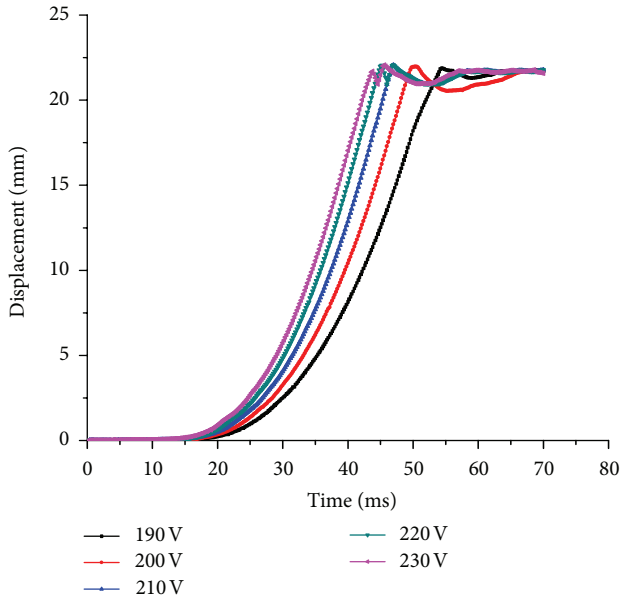


FIGURE 11: Curves without control.

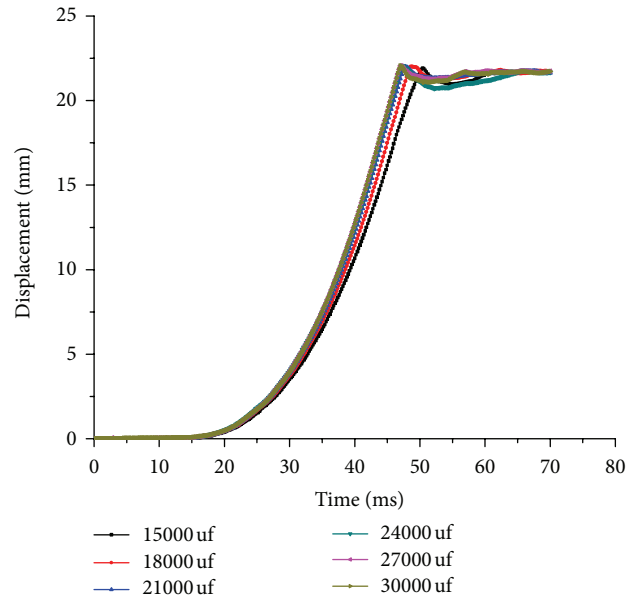


FIGURE 13: Curves without control.

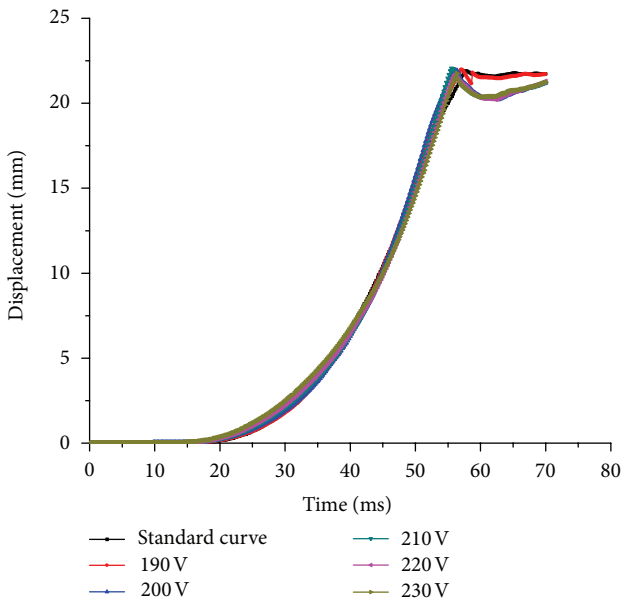


FIGURE 12: Curves controlled.

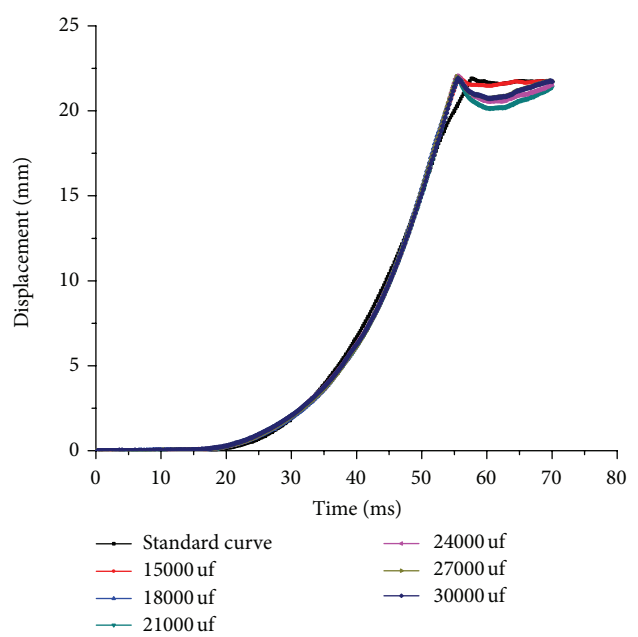


FIGURE 14: Curves controlled.

a certain value, it no longer has effects on the closing speed of iron corn. The capacitor power equals  $(1/2)CU^2$ . It is a linear relationship with the value of capacitance. Therefore, capacitance has a small impact on displacement deviation, which can be easily corrected. According to the adjustment above, larger capacitance should be selected to overcome the time deviation.

**5. Conclusion**

According to the content of this paper, there are four conclusions summarized below.

- (1) In this paper, the research of mathematical method and position control, which is based on the PMA, has been done. Closed-loop system has been established in which free-wheeling process of coil is considered. The discharging and free-wheeling process is analyzed, and the system equations are solved by the method Runge-Kutta. Using the proportional control method and fuzzy algorithm in the simulation system, the given curve can be traced well. The results prove that the method in this paper is effective and this method can guide the practical experiments.

- (2) Experiments have been carried out on prototype in conditions that the voltage changes at intervals of 10 V from 190 V to 230 V and capacitance changes at intervals of 3000  $\mu\text{f}$ . The given curve can be traced well with the algorithm, and the closing time can be stabilized within  $\pm 0.5$  ms while the above factors change.
- (3) With the algorithm proposed in this paper, the deviation of displacement can be corrected very well. Besides, through the experiments, the choice of capacitance value and capacitor voltage value can be guided. The capacitor power also can be fully utilized.
- (4) By the use of this algorithm, displacement deviation can be corrected, and the closing time can be stabilized within  $\pm 0.5$  ms. The lifespan of circuit breaker can be prolonged for the reason that the actuator has a rational closing velocity. The accuracy of phase-controlled operation can also be ensured.

## Acknowledgments

This work was supported by the Fundamental R&D Operating Expenses and Special Projects of Dalian University of Technology (Project no. DUT12LK06) and the National Natural Science Foundation of China (no. 51277019).

## References

- [1] J. P. Dupraz, R. Lüscher, and G. F. Montillet, "A hybrid drive merging a servo-controlled motor and a spring mechanism," *IEEE Transactions on Power Delivery*, vol. 21, no. 2, pp. 640–645, 2006.
- [2] Ma Shaohua, *Research on Permanent Magnetic Actuator of 126kV High Voltage Vacuum Circuit Breaker and Its Synchronous Control Technology*, Shenyang University of Technology, 2008.
- [3] X. Lin, D.-S. Wang, and J.-Y. Xu, "Linear servo motor operating mechanism and control technique for high-voltage circuit breaker," *Proceedings of the Chinese Society of Electrical Engineering*, vol. 28, no. 27, pp. 137–141, 2008.
- [4] E. Dong, T. Qin, Y. Wang, J. Zhao, J. Zou, and X. Chen, "Fuzzy control of a novel magnetic force actuator in 40.5kV SF6 circuit breaker," in *Proceedings of the 1st International Conference on Electric Power Equipment: Switching Technology (ICEPE '11)*, pp. 287–290, Xian, China, October 2011.
- [5] Z. Huang, X. Duan, J. Zou, and M. Chen, "A permanent magnetic actuator with scheduled stroke curve for vacuum circuit breakers," in *Proceedings of the 24th International Symposium on Discharges and Electrical Insulation in Vacuum (ISDEIV '10)*, pp. 162–165, Braunschweig, Germany, September 2010.
- [6] W. Ming, *Research on Adaptive Feedback Control System Based on PWM of Synchronous Switching [M.S. thesis]*, University of Xihua, Hong Kong, China, 2007, DRPT 2004.
- [7] L. Wei, F. Chun-En, Z. Lili et al., "Simulation and testing of operating characteristic of 27.5kV vacuum circuit breaker with permanent magnetic actuator," in *Proceedings of the 23rd International Symposium on Discharges and Electrical Insulation in Vacuum (ISDEIV '08)*, pp. 125–128, Bucharest, Romania, September 2008.
- [8] C. Mingfan, D. Xiongying, H. Zhihui, Z. Jiyan, and D. Enyuan, "Adaptive control for operating time of vacuum switch," *Proceedings of the Chinese Society of Electrical Engineering*, vol. 30, no. 36, pp. 22–26, 2010.
- [9] E. Dong, Z. Zhang, Y. Wang, G. Yin, J. Zou, and X. Chen, "Dynamic characteristic simulation of magnetic force actuator based on Visual Basic interface programming," in *Proceedings of the 1st International Conference on Electric Power Equipment: Switching Technology (ICEPE '11)*, pp. 453–457, Xian, China, October 2011.
- [10] L. Xin, G. Huijun, and C. Zhiyuan, "Magnetic field calculation and dynamic behavior analyses of the permanent magnetic actuator," in *Proceedings of the 19th International Symposium on Discharges and Electrical Insulation in Vacuum*, vol. 2, pp. 532–535, 2000.
- [11] L. Fugui, G. Hongyong, Y. Qingxin et al., "An improved approach to calculate the dynamic characteristics of permanent magnetic actuator of vacuum circuit breaker," *IEEE Transactions on Applied Superconductivity*, vol. 14, no. 2, pp. 1918–1921, 2004.
- [12] Y. Kawase, H. Mori, and S. Ito, "3-D finite element analysis of electrodynamic repulsion forces in stationary electric contacts taking into account asymmetric shape," *IEEE Transactions on Magnetics*, vol. 33, no. 2, pp. 1994–1999, 1997.
- [13] J. H. Kang, C. Y. Bae, and H. kyo J, "Dynamic behavior analysis of permanent magnetic actuator in vacuum circuit breaker," in *Proceedings of the the 6th International Conference on Electrical Machines and Systems*, vol. 1, pp. 100–103, November 2003.
- [14] Z. Guangqi, H. Junan, W. Dong, and L. Chunling, *Fuzzy Control Theory and Its Engineering Applications*, Publishing house of Huazhong University of Science and Technology.
- [15] K.-Y. Cai and L. Zhang, "Fuzzy reasoning as a control problem," *IEEE Transactions on Fuzzy Systems*, vol. 16, no. 3, pp. 600–614, 2008.
- [16] M. Santos, J. M. de la Cruz, S. Dormido, and A. P. de Madrid, "Between fuzzy-PID and PID-conventional controllers: a good choice," in *Proceedings of the Biennial Conference of the North American Fuzzy Information Processing Society (NAFIPS '96)*, pp. 123–127, June 1996.
- [17] L. Jinkun, *MATLAB Simulation of Advanced PID Control*, Electronic Industry Press, Beijing, China, 2nd edition, 2004.
- [18] M. Petrov, I. Ganchev, and A. Taneva, "Fuzzy PID Control of Nonlinear plants," in *Proceedings of the 1st International IEEE Symposium on Intelligent Systems*, vol. 1, pp. 30–35, 2002.





# Hindawi

Submit your manuscripts at  
<http://www.hindawi.com>

